Cellulose (2024) 31:5725–5745
https://doi.org/10.1007/s10570-024-05925-6

ORIGINAL RESEARCH

Construction of nitrate glycerol ether cellulose/RDX energetic composite in gun propellants and its comprehensive performance

Ling Chen · Jianwei Zhang · Derong Meng · Xiang Cao · Binbin Wang · Fengqiang Nan · Feiyun Chen · Ping Du · Xin Liao · Weidong He

Received: 1 July 2023 / Accepted: 19 April 2024 / Published online: 10 May 2024

Abstract In energetic materials, high-energy propellants always encounter poor mechanical properties. Herein, a novel energetic binder nitrate glycerol ether cellulose (NGEC)/hexahydro-1,3,5-trinitro-1,3,5-triazine (RDX) composite was prepared by a facile, safe water suspension and freeze-drying technology, and integrated in gun propellant (GP) through semi-solvent manufacturing. A series of characterizations and tests were conducted to characterize the NGEC/RDX-GP. The findings revealed that the mechanical properties in terms of the impact strength of NGEC/RDX-GPs with different content of NGEC was improved by 15.3%~117.1%, 3.9%~34.6%, 6.9%~31.1% under conditions of -40 °C, 20 °C and 50 °C; the compression strength was improved by 2.5%~23.1%, 10.7%~27.9%, 7.3%~28.5%, while the tensile strength was improved by 15.4%~35.0%, 10.4%~33.0%, 11.8%~35.5%, respectively. Besides, the thermal decomposition dynamics and thermodynamics were also investigated to probe the thermal properties of NGEC/RDX-GP. Moreover, the impact and electrostatic spark sensitivity have also been tested and present excepted results compared with neat propellant. In addition, the improved gunpowder impetus of NGEC/RDX-GP indicated that the energetic performance of propellant was further enhanced, and maintained stable combustion behavior. Finally, the enhancement mechanism of the propellant was discussed and proposed. Therefore, this construction strategy and application of NGEC/RDX composites in propellants can provide reliable fundamental theory and data support for the development of high performances propellant.

Supplementary Information The online version contains supplementary material available at https://doi.org/10.1007/s10570-024-05925-6.

L. Chen · J. Zhang · D. Meng · X. Cao · B. Wang · F. Nan · F. Chen · P. Du · X. Liao · W. He
School of Chemistry and Chemical Engineering, Nanjing University of Science and Technology, Nanjing 210094, Jiangsu, China

L. Chen · J. Zhang · D. Meng · X. Cao · B. Wang · F. Nan · F. Chen · P. Du · X. Liao · W. He
Key Laboratory of Special Energy Materials, Ministry of Education, Nanjing 210094, Jiangsu, China

L. Chen · J. Zhang · D. Meng · X. Cao · B. Wang · F. Nan (✉) · F. Chen · P. Du (✉) · X. Liao · W. He (✉)
National Special Materials Resource Utilization and Green Disposal Technology Innovation Center, Nanjing 210094, Jiangsu, China
e-mail: nfq@163.com

P. Du
e-mail: dp1314@163.com

W. He
e-mail: hewedong@njust.edu.cn

Graphical abstract

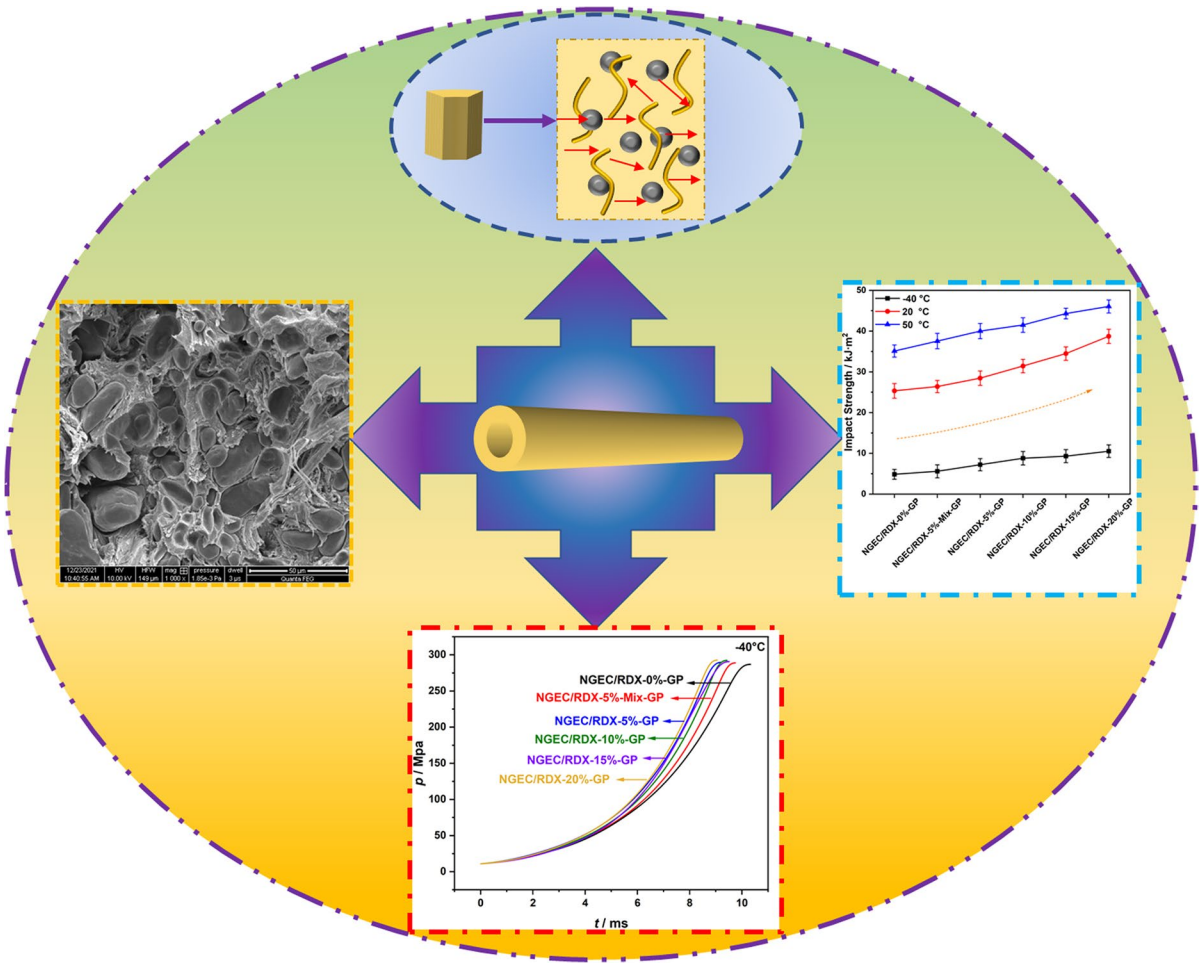

Keywords NGEC/RDX · Gun propellant · Mechanical properties · Thermal decomposition behavior · Combustion

Introduction

Energetic materials (EMs), can typically be classified as propellants, explosives, and pyrotechnics based on their various compositions, properties, and application fields (Chen et al. 2023a; Zhou et al. 2014). Therein, propellants comprising fuels, oxidizers, binders, and functional additives are one significant research aspect of the weapon systems, which produce gases with high temperatures and pressures by controlled combustion behavior and have common applications in rockets and munitions (Liang et al. 2019; Yan et al. 2016). With the development and transformation of weapons and ammunitions, high-energy and high-strength propellants have become an essential direction in the field of propellant technology, in order to ensure the safety performance and energy performance of ammunition (Zhang et al. 2023a, b). Currently, a variety of nitramine explosives like 1,3,5-trinitroperhydro-1,3,5-triazine (RDX, $C_3H_6N_6O_6$), 1,3,5,7-tetranitro-1,3,5,7-tetraazacyclooctane (HMX, $C_4H_8N_8O_8$), and 2,4,6,8,10,12-hexanitro-2,4,6,8,10,12-hexaazaisowurtzitane (CL-20, $C_6H_6N_{12}O_{12}$) have been applied in propellants due to their outstanding energy properties, for instance, the high specific impulse and detonation properties (e.g.,

pressure and velocity) (Groom et al. 2003; Song et al. 2022). Nevertheless, there are still definite drawbacks or limitations existing until now for the application of these high-energy ingredients in propellants. First of all, nitramine explosives usually suffer from high sensitivity toward impact and friction, electrostatic spark, and thermostatic properties etc. It would inevitably produce potential hazardous during the preparation, transportation, store and application, thereby limiting their widely applications. Besides, the addition of solid energy ingredients would decrease the content of polymer binder such as nitrocellulose (NC), resulting in poor mechanical properties of propellants due to the bad adhesive properties between solid ingredients and polymer binder, general named "interface debonding" phenomenon (Chen et al. 2022; Liang et al. 2020; Mulage et al. 2007; Zhenggang et al. 2014). in the ignition and combustion process in a gun chamber, the propellant granules are undertaking very high pressures and pressure gradients quite short times (Li et al. 2015; Luman et al. 2007). This serious situation can even result in mechanical breakup of the propellant granules, and cause a large increase of surface area and so to anomalously high pressurization rates and burning or hazardous breech blow (Shen et al. 2019). Moreover, the crystal transition of several energetic crystals (e.g., HMX: α, β, γ, and σ, and CL-20: α, β, γ, δ, and ε) would weaken the stability of propellants and influence its comprehensive properties, involving the energy, combustion and sensitivity performances (Chen et al. 2021c; Zhang et al. 2020). It is a great challenging to enhance the energy properties at the meantime improving the safety performance of propellants.

Given these reasons, the main research topics to solve above-mentioned problems can be divided into the desensitization research of high-energy explosives, and the study of reinforcing material in improving the mechanical properties of propellants. During the past few decades, the construction strategy of energetic composites could desensitize high-energy explosives effectively by a series of preparation methods, such as sol–gel method, coating method, electrostatic spraying, and mechanical smash technology, etc. Song et al. prepared fluoroelastomers/glycidyl azide polymer/CL-20 (F2602/GAP/CL-20) energetic fibers by the electrospinning method, and the friction sensitivity of F2602/GAP/CL-20 sample in terms of the maximum value was decreased by 38% (Song et al. 2020). Liu et al. obtained several nanometer nitramine explosives RDX, HMX and CL-20 via mechanical smash technology, manifesting the remarkable reduced sensitivity of these products benefiting from its semi-spherical with narrow size distributions and reduced particle size (Liu et al. 2014). Chen et al. synthesized a series of nitrated bacterial cellulose-based energetic nanocomposites by the sol–gel method combined freeze-drying technology, the results indicated that the thermal decomposition performance of the obtained composites was promoted and exerted prominent desensitization effect (Chen et al. 2021a, b, 2020).

Regarding the improvement research in terms of the mechanical properties of propellants, several works show remarkable progress in the past few decades, involving the study of nanoscale reinforcing materials, polymer binder (energetic or not), energetic plasticizer, etc. For example, Shen et al. by utilizing carbon nanofibers (CNFs) (2.0%) and graphene nanoplates (GNPs) (less than 1.0%) to improve the mechanical properties of nitrocellulose (NC) triethylene-glycol-dinitrate (TEGDN)-RDX (NC-TEGDN-RDX)-GP (Chen et al. 2023a, b; Shen et al. 2020, 2019). Wang et al. adopted GAP energetic thermoplastic elastomer (GAP-ETPE) blends as the binder to enhance the compression strength and decrease the mechanical (friction and impact) sensitivity propellants. It has also been proved that GPs containing 2% diglycerol tetranitrate (DGTN) have a better comprehensive mechanical properties comparing with blank sample, wherein the impact strength and compression ratio of the propellant increased by 11.36% and 28% respectively, and the compression strength decreased by 1.9% (Wang et al. 2020). Besides, triethanolamine (TEA) was used by Xu et al. to coat NQ before propellant manufacturing in order to improve the anti-impact strength, the compressive resistance and the extension strength of the modified propellant, which were increased by 44.6%, 20.6% and 7.1% at -40 °C, respectively. Accordingly, these conclusions indicated that constructing energetic composites by a proper method or technology with some desensitizers can effectively reduce the sensitivity of energetic crystals. Meanwhile, via adding some functional nanoscale reinforcing additives, polymer binder could further enhance the mechanical properties of propellants and maintain other comprehensive performance.

Recently, a novel derivative of traditional energetic binder NC, nitrate glycerol ether cellulose (NGEC) has been synthesized and characterized, exhibiting outstanding physicochemical properties (Qing et al. 2012). It is a novel thermoplastic cellulose binder and its appearance is similar to that of NC (Zhang et al. 2014). There are small molecule branch chains in the big molecule main chain of NGEC, which can improve its molecular flexibility and mechanical properties (Zhang et al. 2015). Hence, this kind of energetic binder NGEC exerts potential application in enhancing the mechanical properties of propellants while maintaining the energy performance.

Hence, this research prepared a novel NGEC/RDX composites by a simple, safe method of water suspension and freeze-drying technology, after then, the obtained NGEC/RDX composites were applied into propellants by typical half-solvent method. An increasing trend of mechanical properties can be found with the increasing content of NGEC from 5 to 20%. The study of thermal decomposition performance also demonstrated that integration of NGEC could further enhance the thermal stability of propellant. In addition, the combustion performance of the samples could burn steadily and the energetic performance was improved slightly compared with blank sample. Finally, the sensitivity of samples exerted favorable result in respect of decreasing trend with the increased content of NGEC.

Experimental part

Materials

NGEC (12.6% Nitrogen content) was supplied by laboratory in Beijing Institute of Technology (BIT). RDX (99%, industrial grade) were provided by Liaoning Qing yang Chemical Co., Ltd.; Polyvinyl alcohol (PVA) were provided by Nanjing Aladdin Wanqing Technology Co., LTD. (Shanghai, China). A level of NC (A-NC) with 12.6% nitrogen, NG/NC propellant (41.2/57.8 wt%, and centralite (C_2) (1.0 wt%)) were supplied by Luzhou North Chemical Industry Co., Ltd (Luzhou, China). Ethyl alcohol and ethyl acetate were purchased from Nanjing Chemical Reagent Co., Ltd. (Nanjing, China).

Preparation of NGEC/RDX-GPs

The preparation process of NGEC/RDX-GP with different content of NGEC is displayed in Fig. 1. The detail description is as follow:

Firstly, the basic materials NGEC/RDX were prepared by a simple, safe and efficient water suspension method and freeze-drying technology, via controlling the content of NGEC (5 wt%, 10 wt%, 15 wt% and 20 wt%). The addition of surfactant PVA with mass ratio (RDX: PVA = 20:1) is mainly to modify the surface of RDX crystal by decreasing the surface tension and improve the surface wettability of the energetics, thereby increasing the interaction of composites NGEC/RDX. Then, the obtained suspension solutions were stirring for several hours and ultrasound. Finally, the suspension was centrifugated or vacuum filtration and cleaned with deionized water several times to get rid of impurities. After then, the products were put in cryogenic box (-40 °C) for 30 min, and then placing in low temperature vacuum freeze-dryer at -76 °C for 48 h.

Secondly, the obtained NGEC/RDX composites and the preparative raw materials NC and NG/NC sheets were added into a kneading machine for about 10 min. Meanwhile, a small amount of ethyl alcohol (30 mL) was added into the kneading machine to wet and distribute the pristine materials uniformly, which could also ensure the safety of the EMs during kneading. After 30 min, the mixed solvents consisted of ethyl alcohol and ethyl acetate with volume ratio of 1:1 were added into the kneading machine for further kneading and plasticized with all the ingredients about 3.5 ~ 4 h at 35 °C. After then, the propellant doughs were extruded using two differ extrusion molds (dumbbell-shaped mold and single perforating mold) through a hydraulic press of 60 tons capacity for tensile strengths, compressive strengths and impact properties test. Lastly, all the obtained samples were put into a drying vacuum oven at 40 °C for 7 days to remove the solvent completely. For comparison, the physical mixtures of CNFs and energetic crystals were also prepared with the equal amount of NGEC/RDX-5%-GP. The

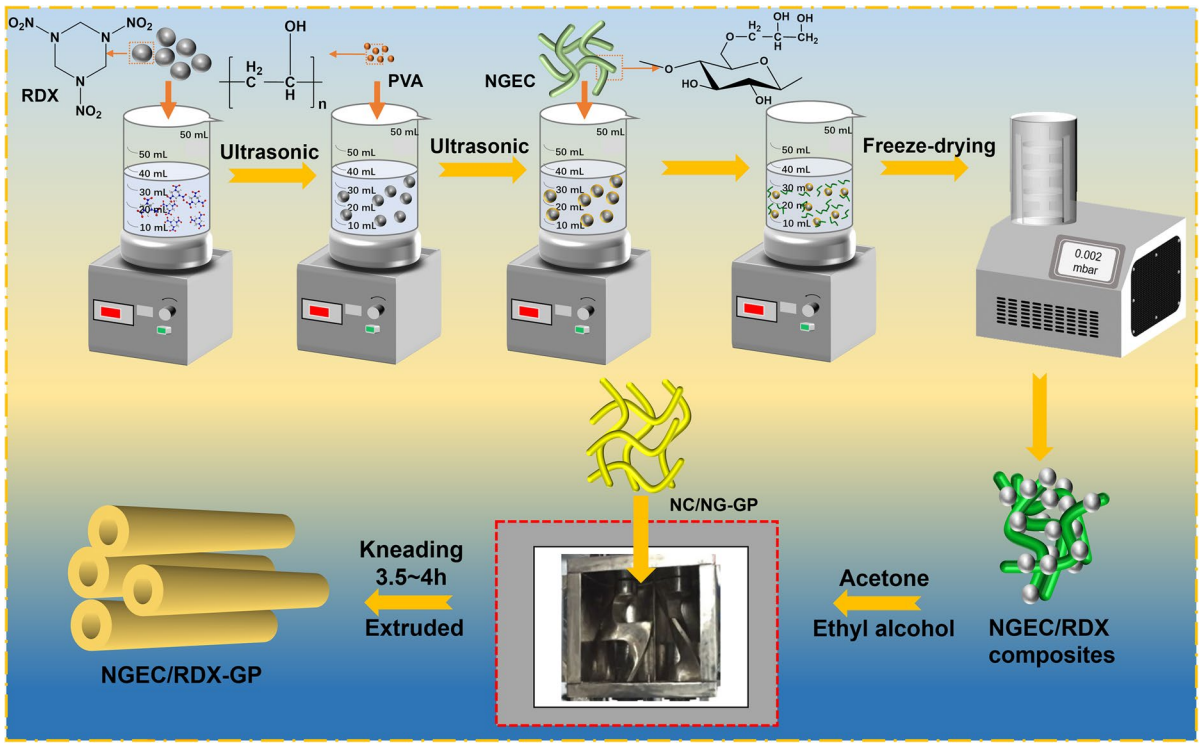

Fig. 1 The diagram description of the preparation process of NGEC/RDX energetic composites and its corresponding NGEC/RDX-GP

formulation of NGEC/RDX-GPs is presented in Table S1.

Characterization

The morphology and dimensions of the microstructure in the composites were observed by a scanning electron microscope (SEM) (FEI, Quanta 250FEG) at an acceleration voltage of 5–10 kV after gold sputtering coating. The structure of GPs were probed by X-ray diffraction (XRD) analysis (Bruker D8 Advanced, Germany), where the diffractometer uses Cu Kα radiation under the conditions of 40 kV and 40 mA, and the scanning range for 2θ is from 10 to 60° at the rate of 0.008°/0.1 s. Fourier transform infrared (FT-IR) (Nicolet iS10, Thermo Scientific, USA) spectroscopy was performed to identify the chemical bonds of the GPs. All spectra were recorded in the 4000–500 cm^{-1} range (resolution 4 cm^{-1}) and by superposing 16 scans. To further study the structure of the as-prepared GPs and disordering degree, the laser microscopy confocal Raman spectrometer (Renishaw inVia 2JGY39) and its corresponding signal mappings of chemistry bonds were also presented under the condition of 532 nm excitation with a 50× objective. To impede the decomposition or ablation of the EMs that could result from the strong laser exposure, which is only controled at a laser power of 10% in each time, the laser beam was set on the as-prepared sample surface for an exposure time of 5 s. The elements of the products was analyzed by X-ray photoelectron spectroscopy (XPS) (Thermo Scientific ESCALAB 250i, USA), accompanied by monochromatic Al Kα X-ray source radiation. The thermal properties were tested by differential scanning calorimetry (DSC) (Netzsch DSC204F1 Phoenix), recording with 40 $mL{\cdot}min^{-1}$ N_2 at 10 $°C{\cdot}min^{-1}$ at the range of 100 °C to 350 °C. (Thermogravimetry-Simultaneous Thermogravimetric Analyze) TG–DTA (STA 8000 instruments) was further carried out to study the thermal performance of GPs at heating rate of 10 $°C{\cdot}min^{-1}$ from 100 °C to 350 °C with N_2 about 20 $mL{\cdot}min^{-1}$. Tensile and compression strengths of the GPs were repeated five

times for each sample in each test condition, and the average values were reported. Therein, the compression strengths testing was conducted by a universal material testing system (American Instron, Model-3367) at across-head speed of 100 mm·min^{-1}, while the tensile tests were carried out on die-cut dumbbellshaped specimens with 5.0–0.5 mm width and 1.0–0.1 mm thickness. Compression tests were conducted on a single perforation grains with a length of 5.0–0.5 mm. The single perforation grains for compression and impact strengths testing were prepared by extrusion mold with an inner and outer diameter of 2–0.1 mm and 5–0.5 mm. The impact strengths tests were conducted on a drop weight impact testing machine (American Instron, Dynatup 9250 HV). The grains were machined to a length of 60 mm. The closed vessel tests performed using a 100 cm^3 vessel reflected a constant volume combustion. A 1.0 g NC powder with 10.98 MPa ignition pressure was used as the ignitor. The loading density of each sample was 0.2 g·cm^3 at -40 °C, 20 °C and 50 °C. In terms of the gunpowder impetus, which was tested with two loading density of each sample about 0.2 g·cm^{-3} and 0.12 g·cm^{-3} at 20 °C. The burning pressure (p), burning time (t), burning rate (u), dynamic vivacity (L), and relative pressure (B) were used to characterize the stability of the combustion (p–t curves), change in burning rate (u-p curves), and combustion state of the burning surface (L-B curves).

In the end, the impact sensitivity was tested by the principle of GJB772A-97 with a fall hammer of OZM research BAM Fall hammer device, and 25 samples with mass of 30 ± 1 mg were tested by drop weight about 2 kg, room temperature of 16 °C, and relative humidity of 15%. The special height (H_{50}) representing the drop height of 50% explosion probability to illustrate the results.

The electrostatic spark sensitivity was tested by an instrument of OZM research Xspark10 tester. The samples were placed between two electrodes discharge with 0.25 mm and initiated by a set voltage. The electrostatic spark energy (E_{ess}) was calculated according to equation:

$$E_{ess} = \frac{1}{2}CU^2 \quad (1)$$

where C is capacitance and U is voltage, E_{ess} was adjusted by set the C and U.

Results and discussion

Morphologies, structure and composition analysis

In Fig. 2, the SEM images displayed the micro-morphological structure of NGEC/RDX-based-GP with different content of NGEC. The morphology of RDX, NGEC and NGEC/RDX-10% is presented in Fig. S2. Benefitting from the kneading force and the extrusion pressure during the propellant manufacturing process, the RDX crystals were dispersed or embedded randomly in the binder matrix. For the blank sample (Fig. 2a), it can be clearly seen that are some structure defects, such as hole and evidence of debonding. It could be observed in the NGEC/RDX-5%-Mix GPs that the interface incompact between RDX and binder matrix as well. For NGEC/RDX-based GP, the SEM images indicated relatively compact interface contact between solid ingredients and binder matrix, and became more evidently with the increasing content of NGEC. Taking NGEC/RDX-5% GP as an example, it could be noticed that the RDX crystals were embedded uniformly and intimately in NC/NGEC binder system. Besides, with the increasing content of NGEC added in propellants, the number of binder fiber morphology became more prominently. However, it seems hard to distinguish the difference of morphology and dimensions in GPs adding NGEC or not, due to the source of NC is also coming from cellulose. It could be only observed that the binder fibers dispersed in GP, there is almost none agglomeration phenomenon of binder fibers in GPs by construction the unique structure of energetic NGEC/RDX composites and applying them in GP. The AFM images (Fig. 3e) displayed the 3D morphology of NGEC/RDX-5% GP, whose roughness was R_q and R_a was 16.8 and 12.7 nm, respectively.

The characterizations of XRD (Fig. 3a), FTIR (Fig. 3b) and Raman (Fig. 3c) are carried out to study the composition and structure of propellant. All samples presented similar characteristic diffraction peaks among each other at 2 degree of in terms of rang from 15° ~ 31° due to the exist of amorphous structure of polymer binder system. Regarding the characteristic diffraction peaks of RDX, which was visible and grew in the swell peak of NC/NG components. Besides, it can be clearly seen that the characteristic diffraction peak of intensity for RDX displayed reduce trend with the increase content of NGEC (Hakey et al. 2008;

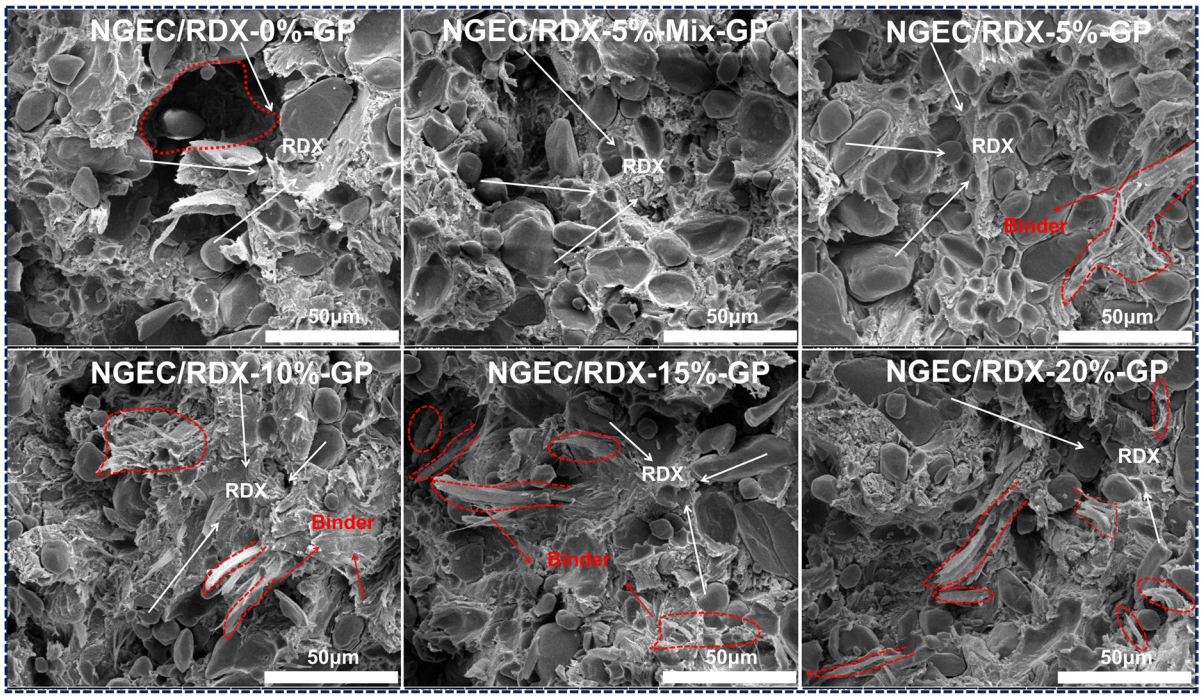

Fig. 2 The SEM images of propellant containing NGEC/RDX

Hultgren 2004). The FTIR spectra analysis demonstrated the structure of propellants was stable. The stretching vibrations of -CH_2 or -CH, anti-symmetry stretching vibration of -NO_2, and C-ONO_2 result from the ingredient NGEC/RDX/NC/NG in propellant system, highlighting that the characteristic peaks of all ingredients were integrated favorably. The Raman spectrum of propellant showed obvious characteristic peak of spectrum. As displayed, a vivid fingerprint-look ring stretching vibration in RDX locating at approximately range from 100 cm^{-1} to 880 cm^{-1}; while the anti-symmetric vibration of -NO_2 are corresponded to the existence of RDX, NC and NG in propellant system in the region of 1210–1600 cm^{-1}. For the characteristic peaks from 2830–3120 cm^{-1} region, which are attributed to the stretching vibration of -CH or -CH_2.

The survey scan XPS spectrums (Fig. 3d) of propellants indicate that the main composition of elements consisting of C, N and O, and the peaks intensity exhibited increase trend with the increase addition of NGEC content, especially O 1 s. Further, high-resolution XPS analysis of NGEC/RDX-GP obtained in the areas of C 1 s, N 1 s, and O 1 s is shown in Fig. 4. The C 1 s spectrum was divided into two disperse peaks, whose binding energies located at approximately 284.8 eV and 287.7 eV that attribute to the existence of C–C and C-H_x, C-O and C-N groups, respectively. Note that the peak intensity of C–C and C-H_x groups showed a decrease trend, while that of C-O and C-N groups displayed the opposite variation with the increased content of NGEC. For N 1 s, it could be generally classified into two peaks at about 401.6 eV and 407.5 eV, assigned to -NO_2 and C-N–C. It should be announced that the peak intensity of -NO_2 and C-N–C groups displayed increase sign with the increased content of NGEC. The similar variation can be observed in the O 1 s region, which was fitted to two sub-peaks at 532.5 eV and 534.2 eV, corresponding to groups of -NO_2 and C–O–C.

Thermal analysis

DSC test was conducted to at different heating rates 5, 10, 15 and 20 $K{\cdot}min^{-1}$ to study the thermal property of propellants, as shown Fig. 5. The thermal parameters are displayed in Table S2 and Table S3. From DSC curves, there are two evident decomposition

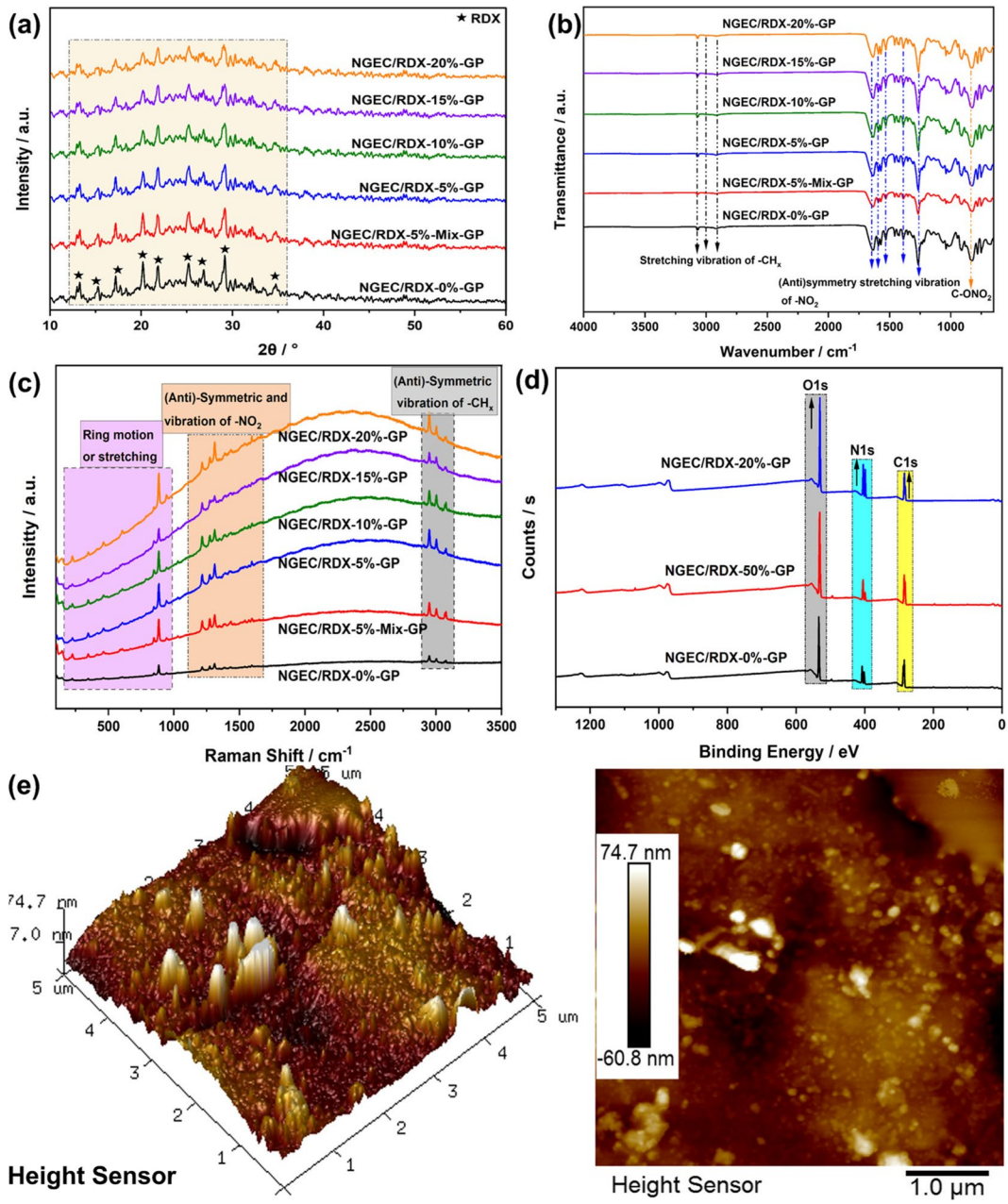

Fig. 3 The XRD patterns (**a**), FT-IR spectra (**b**), Raman spectra (**c**), survey scan XPS spectrums (**d**), and AFM images (**e**) of propellant containing NGEC/RDX

peaks at different heating rates: one main decomposition peak and a relative weak decomposition peak. It could infer that the thermal decomposition of these binder system (NC/NG/NGEC) in propellants leading to the main exothermic peak (197.0 °C ~ 213.4 °C). While the decomposition of RDX crystals at higher temperatures (228.4 °C ~ 246.8 °C) results in the second exothermic peak (Naya and Kohga 2014). As for heat enthalpy of propellant, it was found that propellants added with NGEC was further increased compared with neat propellant in different degree on the whole. Taking NGEC/RDX-5%-GP as an example,

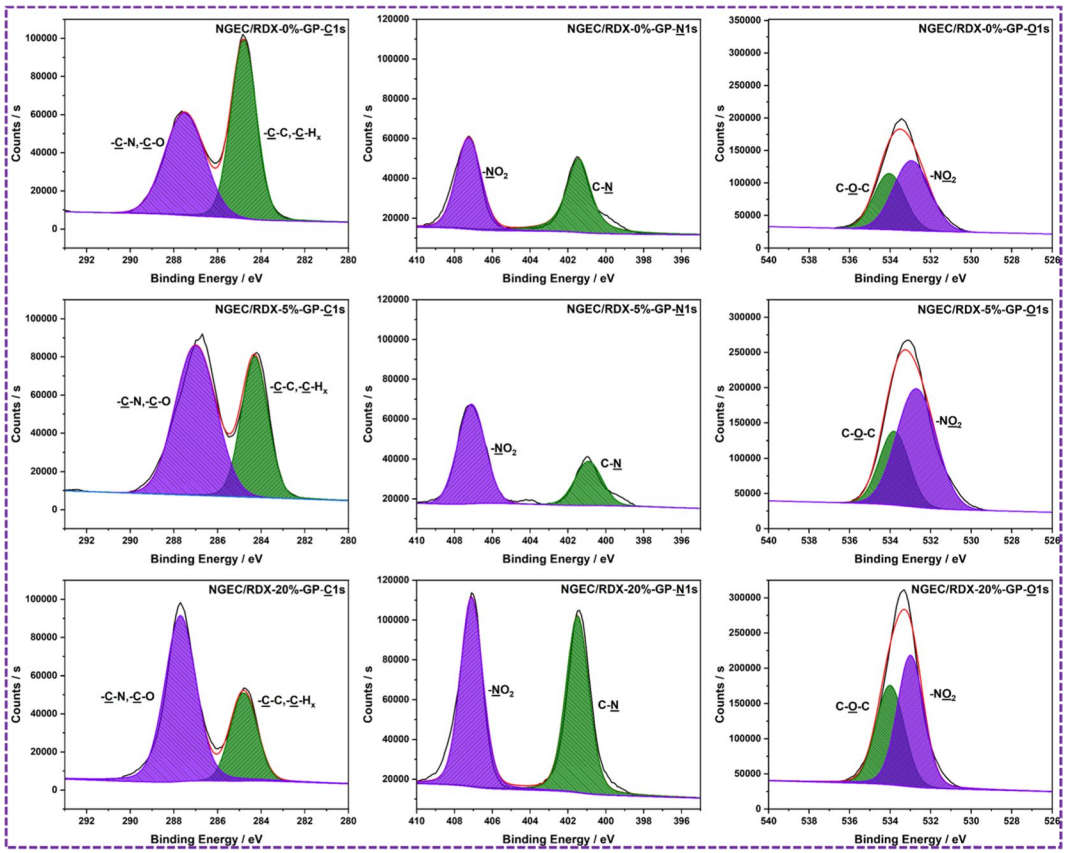

Fig. 4 The high-resolution XPS curves (d) in the areas of C 1 s, N 1 s, and O 1 s of propellant

the heat release at heating rate of 10 K·min^{-1} was increased by 265 J·g^{-1} and 423 J·g^{-1} respectively, comparing with NGEC/RDX-5%-Mix-GP and NGEC/RDX-0%-GP. This phenomenon was more obviously at heating rate 5 K·min^{-1}, where the heat release of blank sample was 491.9 J·g^{-1}, while that of other samples was all more than 900 J·g^{-1}.

Besides, Kissinger method was employed to study the thermal decomposition reaction kinetics and thermodynamics of propellant, and the Ozawa method was performed as a reference for the kinetics study of Kissinger method (Fig. 6). The corresponding parameters are summarized in Table S4 and Table S6, and the activation energy (E_a) was calculated by Eq. (2) (Kissinger) and Eq. (3) (Ozawa), where the parameters β and A_K represent the heating rate and pre-exponential factor.

It can be clearly seen that the E_a obtained by both Kissinger and Ozawa methods presented close results, demonstrating that both methods are suitable for the calculation of thermodynamics of NGEC/RDX-GP. Taking NGEC/RDX-20%-GP as an example, the E_a of first decomposition peak obtained by Kissinger method was 165.90 kJ·mol^{-1}, while that by Ozawa method is 165.34 kJ·mol^{-1}. By comparing E_a of the main decomposition peak of neat propellant and NGEC/RDX-based-GP, it was found that there was slightly decreased phenomenon, indicating that the decomposition process of the propellants was promoted by adding NGEC. It should be noticed that the E_a of the main decomposition peak for NGEC/RDX-5%-GP was larger than that of NGEC/RDX-5%-Mix-GP, and was close to that of neat sample. This outcome also manifested that the construction strategy of NGEC/RDX composites was superior to physical mixing in improving thermal stability of propellants. As for the second decomposition peak, it could be obtained the result that the low addition content of NGEC (5%) exhibited larger E_a (169.4 6 kJ·mol^{-1}/169.23 kJ·mol^{-1}) than that of blank sample (163.15 kJ·mol^{-1}/162.21 kJ·mol^{-1}), while the high one

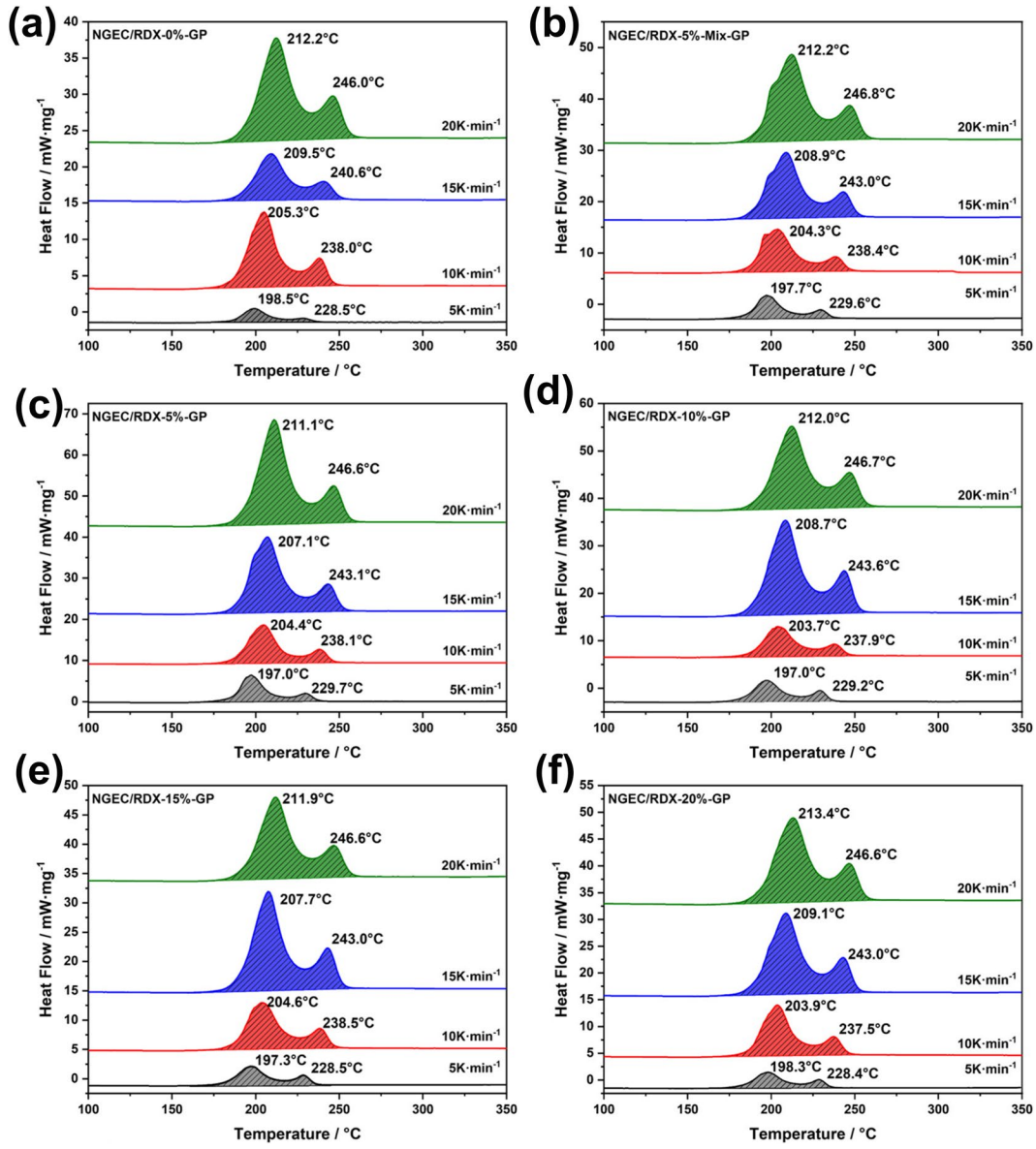

Fig. 5 DSC curves of propellant at heating rate of 5, 10, 15 and 20 K·min.$^{-1}$

exerted decreased outcome. Hence, this phenomenon indicated that the integration of NGEC with suitable content could grant the propellant with favorable heat resistance instead of being activated, and the addition content of 5% may be the best choice.

$$\ln\frac{\beta}{T_P^2} = \ln\frac{R \times A_K}{E_a} - \frac{E_a}{R} \times \frac{1}{T_p} \tag{2}$$

$$\lg \beta = \lg\left[\frac{AE}{RG(\alpha)}\right] - 2.315 - 0.456\frac{E}{RT_p} \tag{3}$$

$$A_K \exp\left(\frac{E_a}{RT_p}\right) = \frac{K_B T_P}{h}\exp\left(-\frac{\Delta G^{\neq}}{RT_p}\right) \tag{4}$$

$$\Delta H^{\neq} = E_{\mathrm{a}} - RT_p \tag{5}$$

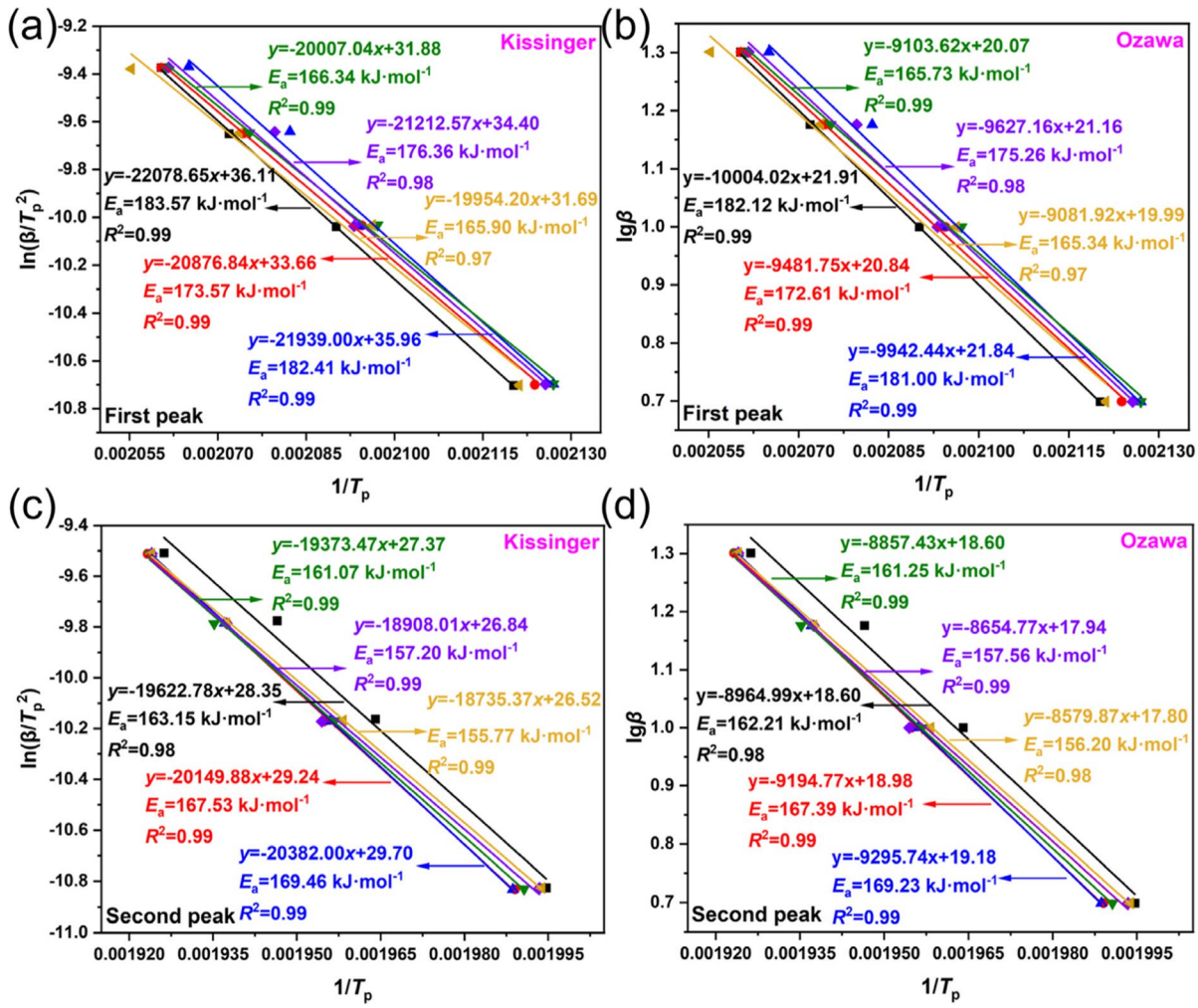

Fig. 6 the E_a calculated by linear fitting methods of Kissinger and Ozawa, (**a**) first peak (**b**) second peak

$$\Delta G^{\neq} = \Delta H^{\neq} - T_p \Delta S^{\neq} \tag{6}$$

$$T_b = \frac{E_a - \sqrt{{E_a}^2 - 4E_a R T_{e0}}}{2R} \tag{7}$$

$$T_{e0} = T_{ei} - b\beta_i - c\beta_i^2 - d\beta_i^3 \tag{8}$$

The thermodynamics parameters like activation enthalpy $\left(\Delta H^{\neq}\right)$, activation free energy $\left(\Delta G^{\neq}\right)$ and activation entropy $\left(\Delta S^{\neq}\right)$ were obtained by Eq. (4)-(6), as displayed in Table S5 and Table S7. The constant parameters of K_B and h are the Boltzmann ($K_B = 1.381 \times 10^{-23}$ J·K^{-1}) and Planck constants (h = 6.626×10^{-34} J·s^{-1}). Theoretically, the decomposition reaction of energetic composites regular follows the decomposition mechanism of single molecular EMs. Nevertheless, the decomposition rate, the broken order of bond or decomposition order of these composite propellants may exert different decomposition behavior. Besides, the obtained propellants consist of both oxidizer (e.g., oxygen elements) and fuel (e.g., carbon elements) or other components, whose decomposition is influenced by the activation and rupture of its relative weak bond. Therefore, the activation process for EMs is very basic and essential, that also dominants the whole decomposition process. It is typically influence by the parameter $\Delta H^{\neq}$, $\Delta G^{\neq}$, and E_a, and $\Delta S^{\neq}$. As can be seen, the $\Delta H^{\neq}$ is highly

intimate to that of E_a, which means the energy that the molecules need absorb from surroundings, is to change the normal state to the activated state. On the whole, the $\Delta H^{\neq}$ of the propellant corresponding to both of the main decomposition peak and the secondary decomposition peak that was very close to the E_a value, indicating that the energy absorbed by the molecule from the surrounding environment is the energy needed to make the normal state into the activated state. For example, the $\Delta H^{\neq}$ of NGEC/RDX-5%-GP is 178.65 kJ·mol^{-1}, while that of E_a is 182.41 kJ·mol^{-1}. Comparing with the physical mixed sample, it shows better thermal stability and is not easy to be activated. For $\Delta G^{\neq}$, it represents the chemical potential of the activation process. According to Table S5, the $\Delta G^{\neq}$ of all propellants has a positive value, indicating that only if enough energy can stimulate the decomposition reaction of the propellant system, thereby the activation reaction process of the propellant system can be developed spontaneously. For instance, the $\Delta G^{\neq}$ of all the propellant samples located at the range from 121 kJ·mol^{-1} to 130 kJ·mol^{-1}, the little differ indicating that the thermal stability of NGEC/RDX based propellant was considerable on the whole, and the NGEC produce little influence on the activation or the difficulty of activation process for propellant system. Regarding $\Delta S^{\neq}$, it is found that the order value of transition state is relatively small for the low activation energy propellant. For example, the $\Delta S^{\neq}$ of NGEC/RDX-20%-GP is 88.85 J·mol^{-1}, while that of NGEC/RDX-5%-GP is 125.40 J·mol^{-1}, which is higher than other propellant samples. In terms of the second thermal decomposition peak, it can be noticed that $\Delta S^{\neq}$ decreased with the increase content of NGEC. However, as far as we know, $\Delta S^{\neq}$ may not be a relative authority, compared with the presence of $\Delta H^{\neq}$ and $\Delta G^{\neq}$, it can still provide a certain reference value for thermodynamic analysis of EMs. The critical temperature of thermal explosion (T_b) is another important thermal performance parameter to evaluate the thermal stability of EMs, which can be calculated from Eq. (7)-(8). The T_b of NGEC/RDX-GP is between 453–464 K. Therein, the T_b of NGEC/RDX-5%-GP was the largest one, which is close to that of neat sample, demonstrating that the proper addition content of NGEC was 5% that could maintain stable thermal stability of propellant.

The calculation of conversion (α), chemical reaction rate and rate constant $k(T)$ were described in supporting information. Figure 7 displays the relationship of α and temperature. It can be found that the α of propellant presented two steps corresponding to the decomposition of NC/NG/NGEC and RDX, and the introduction of NGEC would not influence the α of propellant. The typical iso-conversional rate methods were performed and compared, including Friedman Eq. (9), Ozawa-Flynn-Wall (OFW) Eq. (10), Kissinger–Akahira–Sunose (KAS) Eq. (11) and vyazovkin Eq. (12) for calculations. The expressions of these calculation methods are as follows:

$$\ln\left(\frac{\beta}{T_\alpha^2}\right) = \ln\left(\frac{A_\alpha R}{E_\alpha G(\alpha)}\right) - \frac{E_\alpha}{RT_\alpha} \tag{9}$$

$$\ln \beta = \lg\left(\frac{A_\alpha E_\alpha}{RG(\alpha)}\right) - 2.315 - 0.4567\frac{E_\alpha}{RT_\alpha} \tag{10}$$

$$\ln\left[\left(\frac{d\alpha}{dt}\right)_\alpha\right] = \ln\left[f(\alpha)A_\alpha\right] - \frac{E_\alpha}{RT_\alpha} \tag{11}$$

$$-\ln t = \ln\frac{A}{G(\alpha)} - \frac{E_a}{R}\frac{1}{T} \tag{12}$$

These iso-conversional methods of kinetic analysis can calculate the dependence of $E_a(\alpha)$ and Log$A$ on degree of conversion αwith different constant heating rates β, as shown in Figs. 8 and 9. The corresponding calculation process are displayed in Fig. S3, Fig. S4 and Fig. S5. In Table 1, the average value of E_a $\bar{}$(E_a) and Log$A$ $\bar{}$(Log$A$) for propellant was calculated and summarized to make a clearly contrast among these calculation methods. As displayed, the variation of $\bar{E}_a(\alpha)$ and $\bar{}$Log$A$ calculated by Friedman and Vyazovkin methods displayed similar results, while that of propellant obtained by OFW and KAS methods showed close results. Besides, it was found that the fluctuation of $\bar{E}_a$ and $\bar{}$Log$A$ for neat sample was quite large in the range of α from 0.6 ~ 0.9. However, it became more stable after adding NGEC in propellants, which presented similar variation to that calculated by Kissinger and Ozawa method with the increase content of NGEC. Therein, the $\bar{E}_a$ and $\bar{}$Log$A$ of NGEC/RDX-5% was the largest one comparing to others. In addition, the parameter $\bar{E}_a$ and $\bar{}$Log$A$ of propellant obtained by OFW and KAS methods was larger than that by Friedman and Vyazovkin on the whole. The conversion fitting

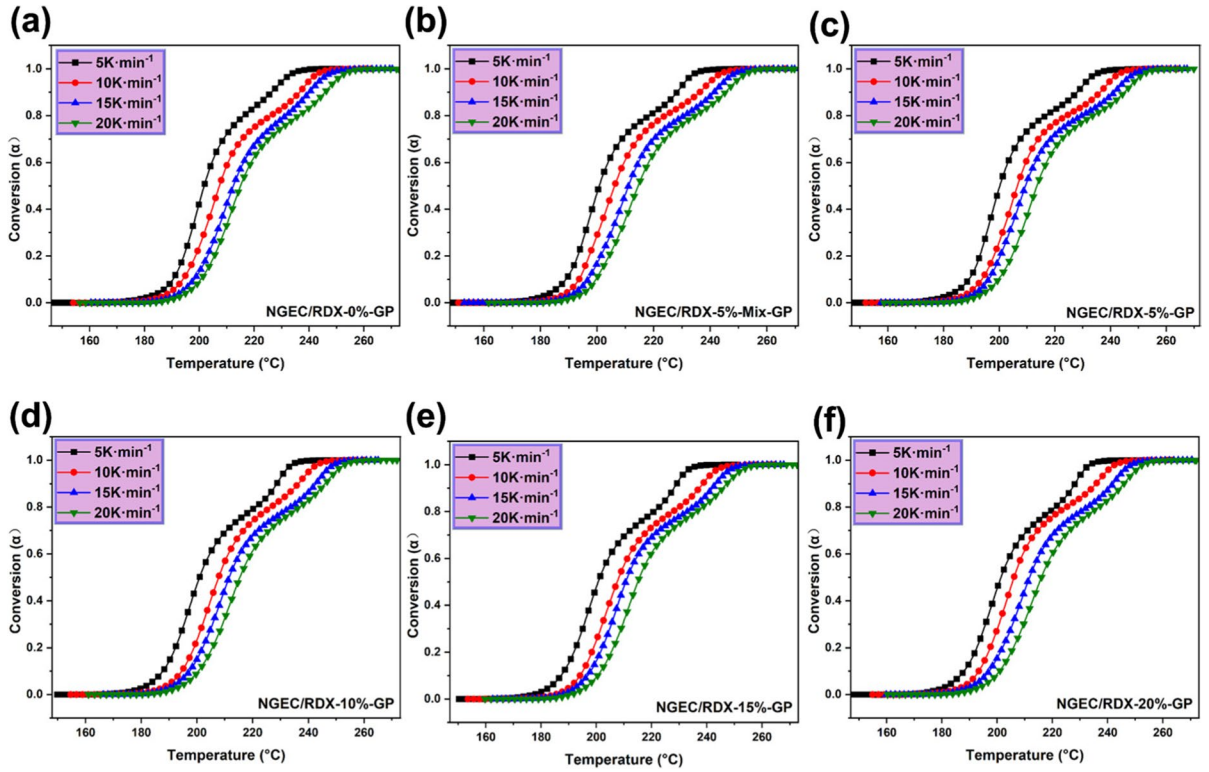

Fig. 7 The variation of conversion for NGEC/RDX-based-GPs

variation of propellant obtained by different methods is displayed in Fig. S6-S11. As can be seen, the fitting degree of conversion by Friedman and Vyazovkin method was better than both methods of OFW and KAS. Therefore, we assume that the iso-conversional methods of Friedman and Vyazovkin should be more suitable for the kinetic analysis of NGEC/RDX-GP.

To further probe the thermal property of propellants, TG and DAT analysis are tested and displayed in Fig. 10a and b, the corresponding thermal parameters are shown in Table S8. It can be observed that there was one main decomposition peak and another weak peak according to the DTA curve of propellants, which was similar to the analysis of DSC curves. The main decomposition peak temperature ranged from 204.78 °C to 206.64 °C, which was ascribed to the decomposition of NC/NG/NGEC in propellant; the second peak ranged from 242.78 °C to 244.96 °C resulting from the decomposition of RDX particles. According to the results of Delta H and the weight loss in Table S8, it can be found that the construction and application of NGEC/RDX composite in propellants exerted violent thermal decomposition performance than that of by physical mixing of NGEC and RDX. For example, the Delta H and the weight loss of NGEC/RDX-5%-GP was 754.67 $J \cdot g^{-1}$ and 83.73%, respectively; while that of NGEC/RDX-5%-GP was 606.48 $J \cdot g^{-1}$ and 79.21%.

Energy performance

For gun propellant, gunpowder impetus was always used to evaluate its energy performance. Herein, the gunpowder impetus of NGEC/RDX-0%-GP, NGEC/RDX-10%-GP and NGEC/RDX-20%-GP is shown in Fig. 10c. As displayed, comparing with blank sample (1190.29 $J \cdot g^{-1}$), the gunpowder impetus value of NGEC/RDX-10%-GP (1201.15 $J \cdot g^{-1}$) and NGEC/RDX -20%-GP (1216.41 $J \cdot g^{-1}$) was much higher. It means the energy performance of propellant was further improved with the increase content of NGEC, demonstrating that the energy level of NGEC is larger than that of NC.

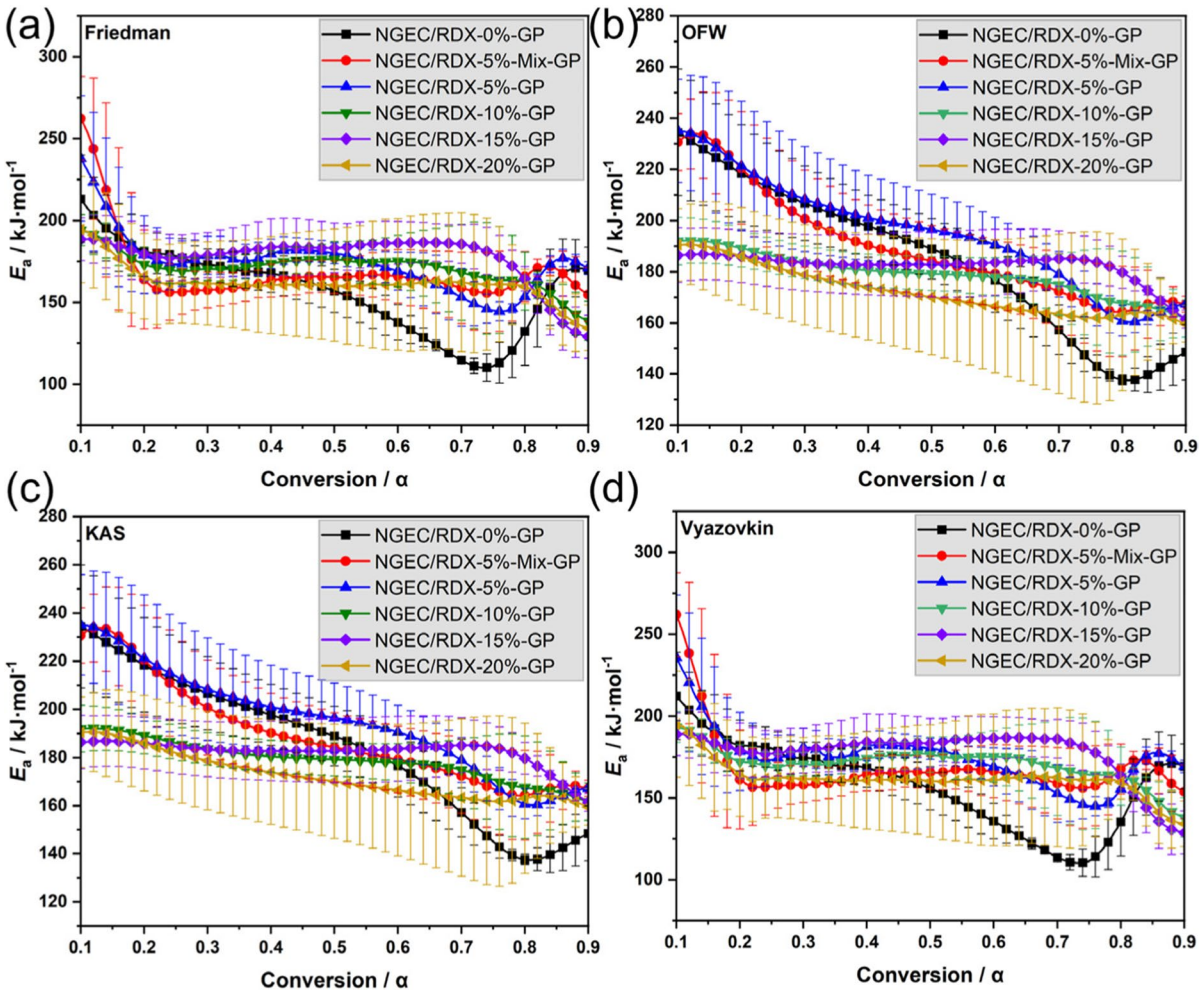

Fig. 8 The variation of E_a following the conversion through calculation method of Friedman (**a**), OFW (**b**), KAS (**c**) and vyazovkin (**d**)

Mechanical properties

Theoretically, temperature has great influence on the mechanical properties of propellants (Shekhar 2011). Moreover, controllable combustion performances and favorable as well as reliable ballistic characteristics are intimately relevant to outstanding mechanical strength of ammunition (Landsem et al. 2012; Wiegand et al. 1990). Therefore, the test of impact strength, tensile strength and compressive strength were performed at -40 °C, 20 °C and 50 °C to study the mechanical properties of propellants, as displayed in Fig. 10d-f. Obviously, a remarkable increasing trend of mechanical strength for NGEC/RDX-GPs could be noticed with the increasing content of NGEC. For example, the impact strength, compressive strength and tensile strength of the NGEC/RDX-0%-GP at -40 °C were 4.85 kJ·m^{-2}, 55.85 MPa and 38.09 MPa, while that of NGEC/RDX-20%-GP was approximately 10.53 kJ·m^{-2}, 68.73 MPa and 51.43 MPa. Moreover, the mechanical properties of the NGEC/RDX-5%-Mix-GP were relative inferior to that of the NGEC/RDX-5%-GP on the whole. For instance, the impact strength, compressive strength and tensile strength of the NGEC/RDX-5%-Mix-GP were 5.59 kJ·m^{-2}, 57.25 MPa and 43.96 MPa at -40 °C, whereas that of the NGEC/RDX-5%-GP were approximately 7.21 kJ·m^{-2}, 60.66 MPa and 45.29 MPa at -40 °C respectively. Another interesting phenomenon could be noticed that the tensile strength

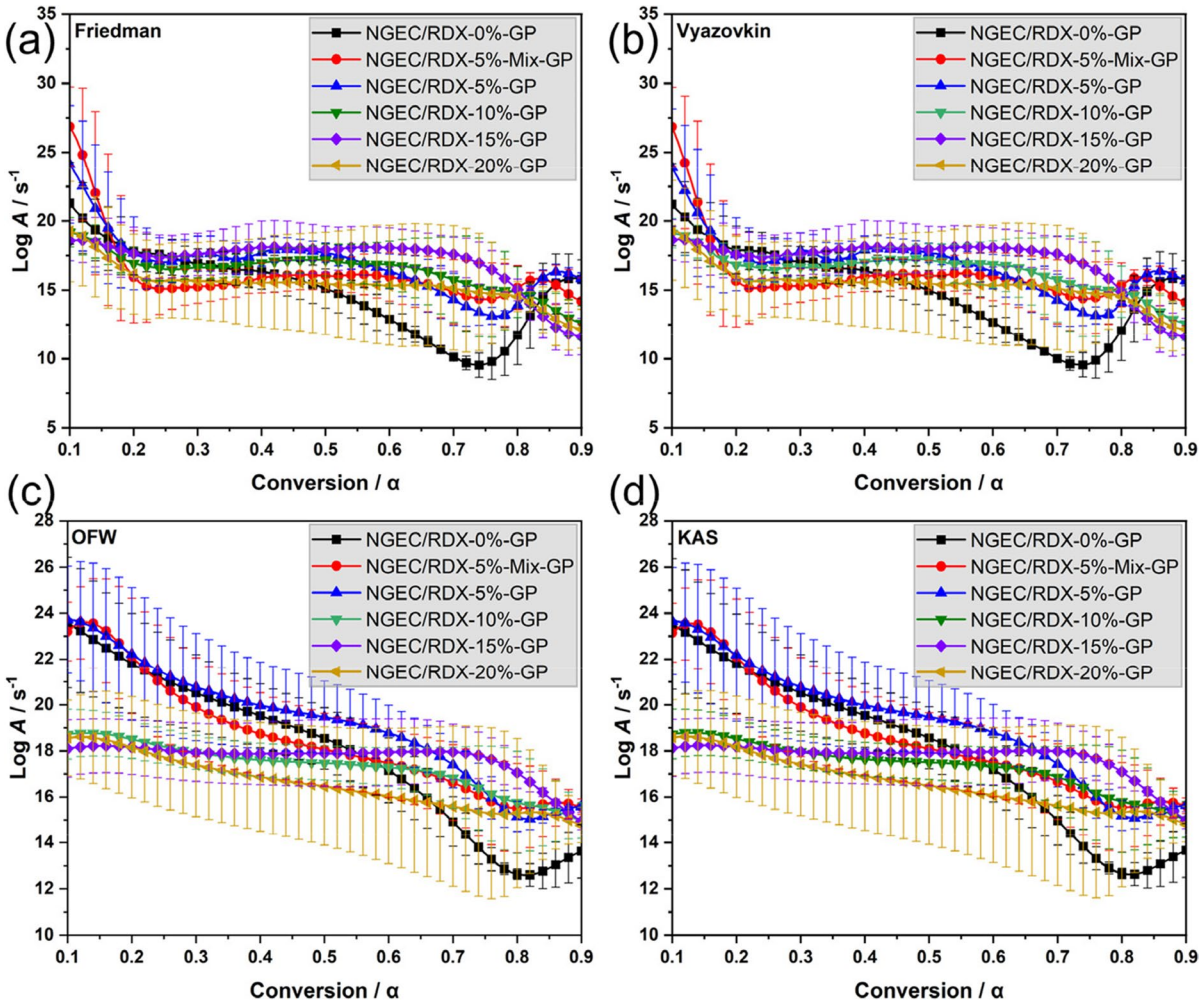

Fig. 9 The variation of Log*A* following the conversion through calculation method of Friedman (**a**), OFW (**b**), KAS (**c**) and vyazovkin (**d**)

Table 1 The $\bar{E}_a$ and $\bar{\text{Log}}A$ calculated by Friedman and Vyazovkin, OFW and KAS methods

Method	Friedman		Vyazovkin		OFW		KAS	
Sample	$\bar{E}_a$ (kJ·mol^{-1})	$\bar{\text{Log}}A$	$\bar{E}_a$ (kJ·mol^{-1})	$\bar{\text{Log}}A$	$\bar{E}_a$ (kJ·mol^{-1})	$\bar{\text{Log}}A$	$\bar{E}_a$ (kJ·mol^{-1})	$\bar{\text{Log}}A$
NGEC/RDX-0%-GP	157.09	15.79	157.38	14.98	184.15	17.94	184.09	17.95
NGEC/RDX-5%-Mix-GP	168.66	16.20	168.41	16.18	189.32	18.53	189.26	18.55
NGEC/RDX-5%-GP	174.58	23.74	174.52	16.88	194.94	19.19	194.88	19.20
NGEC/RDX-10%-GP	170.73	16.38	170.64	16.37	178.85	17.29	178.80	17.32
NGEC/RDX-15%-GP	177.36	17.11	177.22	17.10	182.26	17.68	182.21	17.71
NGEC/RDX-20%-GP	161.88	15.43	161.81	15.43	172.28	16.58	172.21	16.61

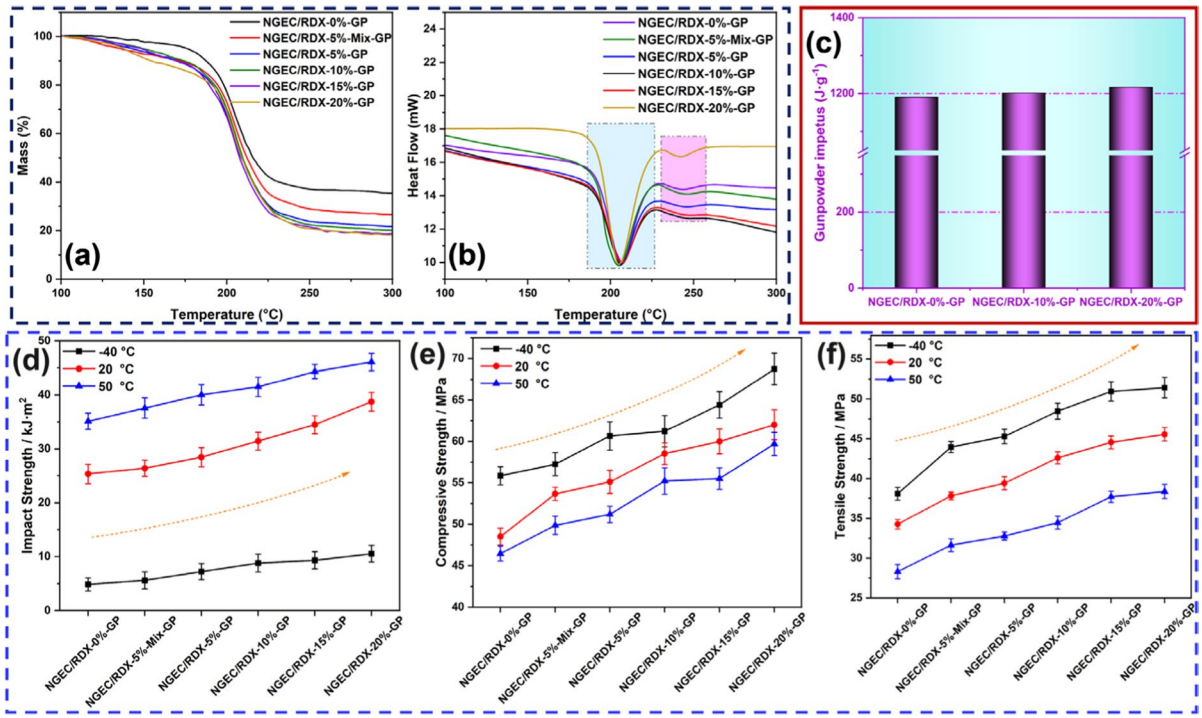

Fig. 10 **a** TG curves, **b** DTA analysis, **c** gunpowder impetus, **d** anti-impact strength, **e** anti-compressive strength, **f** anti-tensile strength of NGEC/RDX-GP

and compressive strength at -40 °C were higher than that at 50 °C, whereas the impact strength exhibited opposite trend. The main reason could be ascribed to the polymer matrix becomes hard with decreasing temperature. It means that propellants undergo a physical transition from a ductile to brittle as temperature begins to drop, similar to a glass transition temperature in polymers (Parker et al. 2016). This transition may occur in the temperature region from 50 °C (ductile) to -40 °C (brittle). Nevertheless, note that an evident phenomenon could be seen that the increased trend of tensile strength seemed to be slightly weaken, when the addition content of NGEC reached 15%, as shown in Fig. 10f. Therefore, a proper addition content of NGEC combined the construction strategy of NGEC/RDX composites could effectively enhance the impact, tensile and compressive strength of the propellant.

Combustion performance

In Fig. 11, the influence of NGEC on the burning characteristic of propellant was evaluated under conditions of -40 °C, 20 °C and 50 °C by the typical test method of closed bomb vessel. The burning rate (u) and burning pressure (p) of the propellant are calculated by Vieille's principle basing on Eq. (12) (Kubota 2002; Oberle 2001; Trache et al. 2019). Therein, the parameter a in Eq. (12) represents the burning rate coefficient, which is a constant dependent on the chemical composition and the initial propellant temperature; while n represents the pressure exponent of u. The dynamic vivacity (L) and relative pressure (B) can be obtained by Eqs. (13) and (14) (Li et al. 2014; Xiao et al. 2016; Chen et al. 2024).

$$u = ap^n \tag{13}$$

$$L = \frac{\mathrm{d}p(t)/\mathrm{d}t}{p(t) * p_\mathrm{m}} \tag{14}$$

$$B = \frac{p(t)}{P_\mathrm{m}} \tag{15}$$

From p–t curves in Fig. 11a-c, it can be seen that the p of propellant added NGEC reaches their

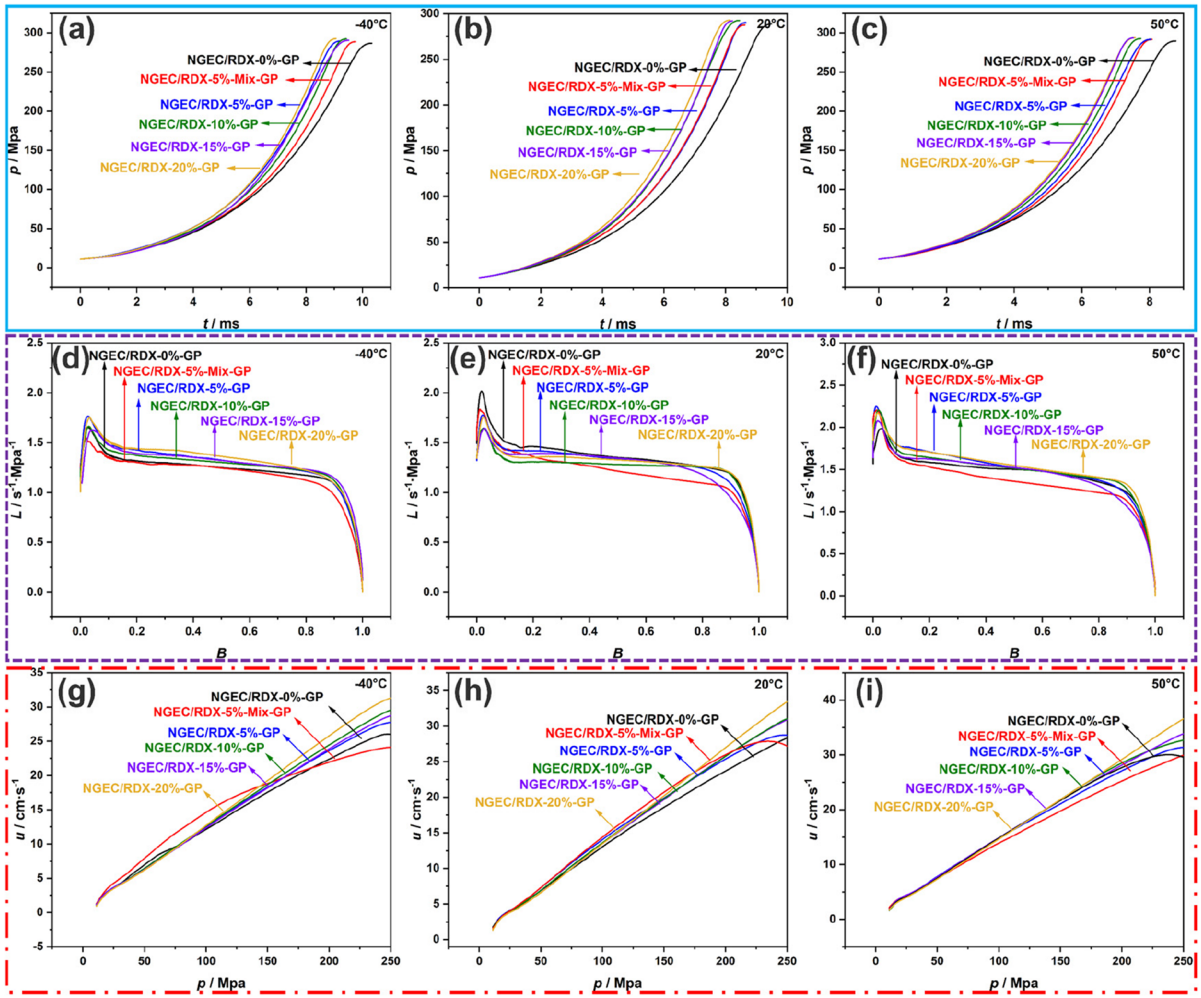

Fig. 11 The *p–t* (**a-c**), *L-B* (**d-f**) and *u-p* (**g-i**) curves at -40 °C, 20 °C and 50 °C of NGEC/RDX-GP with different mass fraction of CNFs

maximum value by less time than that of the neat sample under different temperature conditions. Besides, the maximum pressure (p_m) of NGEC/RDX-GP is also larger than that of the neat sample, as shown in Fig. 12a. This is because NGEC is an excellent energetic binder which is able to produce huge amounts of gases and releases a lot of heat in the burning process comparing with NC.

L-B curves relationship has always been used to assess the geometric progressivity of propellants and to estimate the burning regularly stability (Xiao et al. 2016). As displayed in Fig. 11d-f, all samples can be steadily burned under different temperature conditions according to the smoothly burning characteristic analysis without any distinct abnormal combustion phenomenon. Furthermore, the regressively burning behavior of propellant can be noticed in the *L-B* curves, this phenomenon is consistent with the regressive combustion behavior of one-perforation grain propellant in theory (Shen et al. 2020). It means that the addition of NGEC has almost none influence on the stable combustion performance of propellant.

The *u* is an essential parameter that can be varied by adjusting the propellant ingredients. Meanwhile, the burning rate is also the key element in complex geometry design and interior ballistic design (Yang et al. 2020). In Fig. 11g-i, it can be observed that the *u* of propellant was increased after

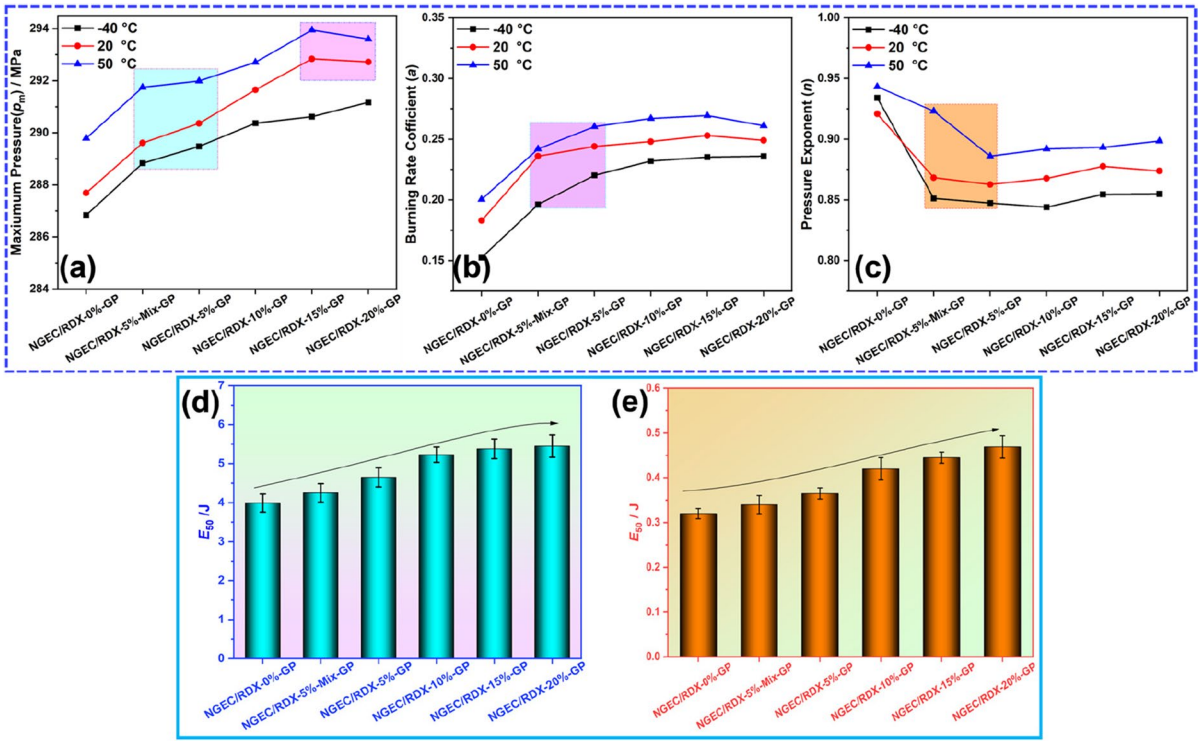

Fig. 12 **a** maximum pressure, **b** burning rate coefficient, **c** pressure exponent, **d** impact and **e** electrostatic spark sensitivity of NGEC/RDX-GP

adding NGEC, and exhibited increased trend with the increasing content of NGEC.

To furtherly study the variation regular of combustion parameters of propellants in burning process. The variation of *a* and *n* of propellants with different addition contents of NGEC are displayed in Fig. 12b and c, respectively. As displayed, the *a* and *n* presented opposite variation trend respectively when the addition contents of NGEC were low, and this variation became slightly when the addition contents of NGEC reached 10% and 15%. Comparing the results of *a* and *n* of NGEC/RDX-5-Mix-GP and NGEC/RDX-5-GP, the combustion stability of NGEC/RDX-GP is better than that of by physical mixing of RDX and NGEC in propellant. On another hand, based on Eq. (12), which indicated that the *p*, *n* and *a* are intimately interactive and tangled, almost slight change in any of the experimentally measured variables can lead to evidently variations in the calculated *a* or *n*. These above-mentioned results revealed that the moderate content of NGEC (10%-15%) could be used as an excellent energetic binder to modify the combustion performance of the propellants.

Sensitivity performance

The test of impact and electrostatic spark sensitivities were performed to investigate the safety performance of propellants, as shown in Fig. 12d and e. As displayed, the NGEC/RDX-GP exerted remarkable desensitization effect compared to neat sample. The maximum increment of impact energy and electrostatic ignition energy of propellant could reach 36.6% and 46.6% respectively. The sensitivity of propellant presented a decrease trend with the increase addition of NGEC content. However, this increasing trend weakened slightly when the addition of NGEC contents reached 15%. It revealed that the integration of NGEC has a positive effect on reducing the sensitivity of propellants, and 15% addition of NGEC may be a favorable threshold value in this study. Besides, comparing with NGEC/RDX-5%-Mix-GP, the construction of energetic NGEC/RDX composites also

exhibited the superiority performance in reducing the sensitivity of propellant.

The proposed mechanism of enhanced mechanical performance

Based on the mechanical properties results, the possible enhanced mechanism of mechanical properties for NGEC/RDX-GP is proposed In Fig. 13. In theory, the mechanical strength of traditional propellant mainly comes from the skeleton supporting structure of NC binder matrix. When the high-energy solid filler is introduced into the binder matrix, which exists in the matrix in random dispersion and embedded or trapped way. Once subjecting to the load force, the stress concentration leads to the pores or voids in the microstructure of the propellant, that weakens the interface interaction between the matrix and the filler, resulting in RDX peeling off the matrix, as well as forming phenomenon of "interface debonding". In this study, the mechanical properties of NGEC/RDX composites were enhanced through the construction and application of NGEC/RDX composites in propellant, which can be divided into NGEC molecular flexibility toughening and micro-interface strengthening of propellant. Firstly, compared with NC, the molecule main chain of NGEC has multi-carbon small molecular branch chain, which has better toughness and plasticity, lower rigidity, and better compatibility with NG. Secondly, the compactness of the filler and binder system in the composite system is better, due to NGEC/RDX composites have better uniform dispersion compared with blank sample, and there is a close interaction between RDX and NGEC. Under different temperature conditions, when the propellant is subjected to radial load force, the flexibility of NGEC molecules grants the propellant with stronger fracture resistance. In addition, in the extrusion process of the propellant, NGEC/NC matrix is mainly arranged in an axial manner due to the extrusion mechanical force. Therefore, the anti-impact strength of the propellant increases more obviously under the action of radial external force. Under axial loading, the better solubility and plasticization degree of NGEC molecules with NG are conducive to the formation of a better continuous phase. The intermolecular force of the composite system can dissipate part of the stress stimulus, reduce the phenomenon of stress concentration, decrease the possibility of micro-cracks at the interface between RDX and the binder in the microstructure, and slow down the crack growth trend. The removal and shedding of RDX from the polymer matrix are relieved, which gives the propellant better axial tensile and compressive resistance. Therefore, the excellent mechanical strength of NGEC/RDX-GP is resulted from the synergistic effect of NGEC molecule flexibility toughening and composite interface strengthening.

Conclusion

In summary, this research introduced a design and application strategy of energetic NGEC/RDX composites in

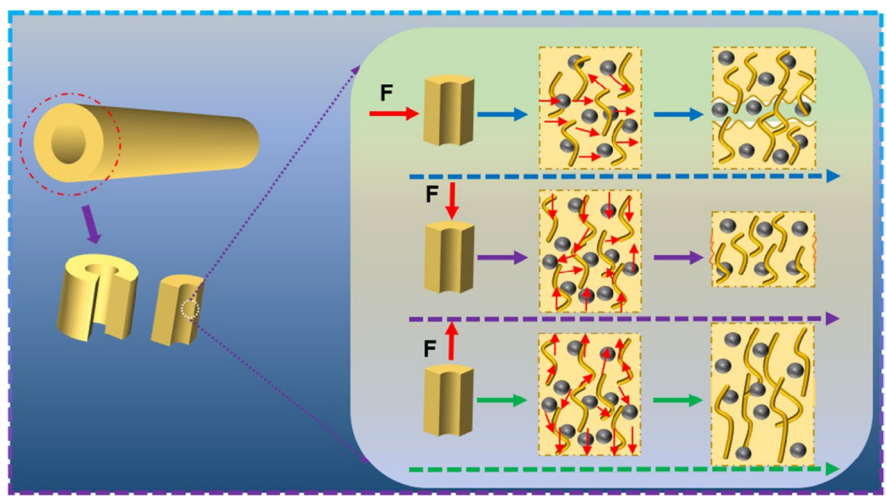

Fig. 13 The proposed mechanism of enhanced strength for NGEC/RDX-GP

propellant. It was found that the mechanical properties of propellants were improved remarkably. Comparing with neat sample, the impact strength of NGEC/RDX-GPs with different content of NGEC was improved by 15.3%~117.1%, 3.9%~34.6%, 6.9%~31.1% under conditions of -40 °C, 20 °C and 50 °C; the compression strength was improved by 2.5%~23.1%, 10.7%~27.9%, 7.3%~28.5%, while the tensile strength was improved by 15.4%~35.0%, 10.4%~33.0%, 11.8%~35.5%, respectively. Besides, the thermal decomposition dynamics and thermodynamics were also investigated and demonstrated the addition of NGEC with content 5% exerting better thermal stability. It was proved that the iso-conversional methods of Friedman and Vyazovkin are more suitable for the kinetic analysis of NGEC/RDX-GP. Moreover, the safety performance of propellant was enhanced since the favorable desensitization effect of impact and electrostatic spark sensitivities. Meanwhile, the energy performance of propellant was further enhanced by adding NGEC. Hence, this construction strategy and performance of NGEC/RDX-GP can offer a promising application of NGEC-based composites in high-strength and high-strength propellants.

Acknowledgments This study thanks to Professor Zeshan Wang, Professor Bin Xu, Professor Zhitao Liu, Engineer Yu Yannian, Engineer Yin Shenglai for their experimental help and technical support. Thanks to the analysis and testing center of Nanjing university of science and technology for their experimental help and technical supporting.

Author contributions Ling Chen: Data curation, Methodology, Writing-Original draft preparation. Jianwei Zhang: Reviewing and Writing. Derong Meng: Data curation. Xiang Cao: Writing-Editing. Binbin Wang: Reviewing and Writing. Fengqiang Nan: Supply for the experimental platform, funding provider, Writing-Editing. Feiyun Chen: Supply for the experimental. Ping Du: Reviewing, Funding acquisition. Xin Liao: Writing-Reviewing and Editing. Weidong He: corresponding author, Conceptualization, Raw materials provider, Writing-Reviewing and Editing, Funding acquisition.

Funding This work thanks to the supporting of Jiangsu Funding Program for Excellent Postdoctoral Talent (2023ZB472), and Project funded by China Postdoctoral Science Foundation (2023TQ0158). This research was supported by the National Funding Postdoctoral Researcher Program (GZC20233496).

Data availability Data and materials can be obtained on quest from authors by email.

Declarations

Ethics approval and consent to participate Not applicable.

Consent for publication All the authors listed have approved the enclosed manuscript for publication.

Competing interests The authors declare no competing interests.

References

Chen L, Cao X, Gao J, He W, Liu J, Wang Y, Zhou X, Shen J, Wang B, He Y et al (2021a) Nitrated bacterial cellulose-based energetic nanocomposites as propellants and explosives for military applications. ACS Appl Nano Mater 4:1906–1915

Chen L, Cao X, Gao J, Wang Y, Zhang Y, Liu J, He W (2021b) Synthesis of 3D porous network nanostructure of nitrated bacterial cellulose gel with eminent heat-release, thermal decomposition behaviour and mechanism. Propellants Explos Pyrotech 46:1292–1303

Chen L, He W, Liu J (2020) Safe fabrication, thermal decomposition kinetics, and mechanism of nanoenergetic composite NBC/CL-20. ACS Omega 5:31407–31416

Chen L, Li Q, Zhao L, Nan F, Liu J, Wang X, Chen F, Shao Z, He W (2022) Enhancement strategy of mechanical property by constructing of energetic RDX@CNFs composites in propellants, and investigation on its combustion and sensitivity behavior. Combust Flame 244:112249

Chen L, Mao X, Li Q, Cao X, Zhang J, Wang Y, Liu J, He W (2021c) One-step, safe and efficient preparation strategy of nitrate glycerol ether cellulose-based energetic composites with application potential in propellants. Compos Commun 28:100956

Chen L, Meng D, Zhang J, Cao X, Nan F, Liao X, He W (2023a) Bio-inspired designing strategy and properties of energetic crystals@ (CNFs@PDA) composites. Cellulose 30:7729–7743

Chen L, Sun A, Meng D, Wang B, Chen F, Nan F, Du P, He W (2024) Modified mechanical strength, thermal decomposition, and combustion characteristics of nitroguanidine propellant with graphene nanosheets as reinforcement. Ind Eng Chem Res 63(13):5527–5541

Chen L, Wang B, Zhang J, Meng D, Nan F, Du P, Liao X, He W (2023b) Comparison of the structure and thermal properties of energetic binders for application in propulsion. ACS Appl Polym Mater 5:9103–9115

Groom CA, Halasz A, Paquet L, D'Cruz P, Hawari J (2003) Cyclodextrin-assisted capillary electrophoresis for determination of the cyclic nitramine explosives RDX, HMX and CL-20: comparison with high-performance liquid chromatography. J Chromatogr A 999:17–22

Hakey P, Ouellette W, Zubieta J, Korter T (2008) Redetermination of cyclo-trimethyl-ene-trinitramine. Acta Crystallogr Sect E Struct Rep Online 64:o1428

Hultgren R (2004) An X-ray study of symmetrical trinitrotoluene and Cyclo trimethylenetrinitramine. J Chem Phys 4:84–84

Kubota N (2002) Propellants, explos. Wiley-VCH

Landsem E, Jensen TL, Hansen FK, Unneberg E, Kristensen TE (2012) Mechanical properties of smokeless

composite rocket propellants based on prilled ammonium dinitramide. Propellants Explos Pyrotech 37:691–698
Li Y, Yang W, Ying S (2014) Preparation and characteristics of foamed nc-based propellants. Propellants Explos Pyrotech 39:677–683
Li Y, Yang W, Ying S, Peng J (2015) Combustion of gas-permeable gun propellants. J Energ Mater 33:167–179
Liang T, Qi L, Ma Z, Xiao Z, Wang Y, Liu H, Zhang J, Guo Z, Liu C, Xie W et al (2019) Experimental study on thermal expansion coefficient of composite multi-layered flaky gun propellants. Compos B 166:428–435
Liang T, Zhang Y, Ma Z, Guo M, Xiao Z, Zhang J, Dong M, Fan J, Guo Z, Liu C (2020) Energy characteristics and mechanical properties of cyclotrimethylenetrinitramine (RDX)-based insensitive high-energy propellant. J Mater Res Technol 9:15313–15323
Liu J, Jiang W, Yang Q, Song J, Hao G-Z, Li F-S (2014) Study of nano-nitramine explosives: preparation, sensitivity and application. Def Technol 10:184–189
Luman JR, Wehrman B, Kuo KK, Yetter RA, Masoud NM, Manning TG, Harris LE, Bruck HA (2007) Development and characterization of high performance solid propellants containing nano-sized energetic ingredients. Proc Combust Inst 31:2089–2096
Mulage KS, Patkar RN, Deuskar VD, Pundlik SM, Kakade SD, Gupta M (2007) Studies on a novel thermoplastic polyurethane as a binder for extruded composite propellants. J Energ Mater 25:233–245
Naya T, Kohga M (2014) Influences of particle size and content of RDX on burning characteristics of RDX-based propellant. Aerosp Sci Technol 32:26–34
Oberle W (2001) Dynamic vivacity and its application to conventional and electrothermal-chemical (ETC) closed chamber results. Engineering, Physics 57
Parker S, Reit R, Abitz H, Ellson G, Yang K, Lund B, Voit WE (2016) High-Tg thiol-click thermoset networks via the thiol-maleimide Michael addition. Macromol Rapid Commun 37:1027–1032
Qing XU, Si-yu X, Feng-qi Z, Jian-hua Y, Hong-xu G, Ziqiang S, Hai-xia H (2012) Thermal behavior and thermal safety of nitrate glycerol ether cellulose. Chem Res Chin Univ 28:516–519
Shekhar H (2011) Effect of temperature on mechanical properties of solid rocket propellants. Def Sci J 61:529–533
Shen J, Liu Z, Xu B, Chen F, Zhu Y, Fu Y, Kline DJ, Liao X, Wang Z (2020) Tuning the thermal, mechanical, and combustion properties of NC-TEGDN-RDX propellants via incorporation of graphene nanoplates. J Energ Mater 38:326–335
Shen J, Liu Z, Xu B, Liang H, Zhu Y, Liao X, Wang Z (2019) Influence of carbon nanofibers on thermal and mechanical properties of NC-TEGDN-RDX triple-base gun propellants. Propellants Explos Pyrotech 44:355–361
Song S, Tian X, Wang Y, Qi X, Zhang Q (2022) Theoretical insight into density and stability differences of RDX, HMX and CL-20. CrystEngComm 24:1537–1545
Song X, Guo K, Wang Y, Li F (2020) Characterization and properties of F 2602 /GAP/CL-20 energetic fibers with high energy and low sensitivity prepared by the electrospinning method. ACS Omega 5:11106
Trache D, Maggi F, Palmucci I, DeLuca LT, Khimeche K, Fassina M, Dossi S, Colombo G (2019) Effect of amide-based compounds on the combustion characteristics of composite solid rocket propellants. Arab J Chem 12:3639–3651
Wang Y, Yang H, Han J, Gao K (2020) Effect of DGTN content on mechanical and thermal properties of modified single-base gun propellant containing NQ and RDX. Propellants Explos Pyrotech 45:128–135
Wiegand DA, Nicolaides S, Pinto J (1990) Mechanical and thermomechanical properties of NC base propellants. J Energ Mater 8:442–461
Xiao Z, Ying S, Xu F (2016) Progressive burning performance of deterred oblate spherical powders with large web thickness. Propellants Explos Pyrotech 41:154–159
Yan Q-L, Zhao F-Q, Kuo KK, Zhang X-H, Zeman S, DeLuca LT (2016) Catalytic effects of nano additives on decomposition and combustion of RDX-, HMX-, and AP-based energetic compositions. Prog Energy Combust Sci 57:75–136
Yang W, Hu R, Zheng L, Yan G, Yan W (2020) Fabrication and investigation of 3D-printed gun propellants. Mater Des 192:108761
Zhang J, Chen L, Yang J, Bian C, He W (2023a) Thermal behaviors, thermal decomposition mechanism, kinetic model analysis and thermal hazard prediction of 3,6,7-triamino-7H-[1,2,4]triazolo[4,3-b][1,2,4]triazole (TATOT). Thermochim Acta 724:179515
Zhang J, Chen L, Zhao L, Jin G, He W (2023b) Experimental insight into interaction mechanism of 1H-tetrazole and nitrocellulose by kinetics methods and TG-DSC-FTIR analysis. J Anal Appl Pyrolysis 169:105853
Zhang M, Tan Y, Zhao X, Zhang J, Huang S, Zhai Z, Liu Y, Yang Z (2020) Seeking a novel energetic co-crystal strategy through the interfacial self-assembly of CL-20 and HMX nanocrystals. CrystEngComm 22:61–67
Zhang Y, Shao Z, Gao K, Wu X, Liu Y (2014) Tensile properties of nitrate glycerol ether cellulose/graphene oxide nanocomposites. Integr Ferroelectr 154:147–153
Zhang Y, Shao Z, Li J, Gao K, Liu Y (2015) Aerogel of nitrate glycerol ether cellulose based on phase separation in acetone/ethanol mixed solvents system. J Appl Polym Sci 132(5):41405
Zhenggang X, He W, Ying S (2014) Current trends in energetic thermoplastic elastomers as binders in high energy insensitive propellants in China. Sci Technol Energ Mater 75(1–2):37–43
Zhou X, Torabi M, Lu J, Shen R, Zhang K (2014) Nanostructured energetic composites: synthesis, ignition/combustion modeling, and applications. ACS Appl Mater Interfaces 6:3058–3074